Optica Applicata, Vol. XLVII, No. 3, 2017
DOI: 10.5277/oa170306

Erbium-doped fiber ring laser dynamical analysis for chaos message masking scheme

S. ZAFAR ALI[1], M. KHAWAR ISLAM[2*]

[1]Department of Electrical Engineering, Air University, E-9 Islamabad, Pakistan

[2]Department of Electrical Engineering, Taibah University, Al Madinah Al Munawarah, Kingdom of Saudi Arabia

[*]Corresponding author: drmkislam@gmail.com

A detailed dynamical analysis of erbium-doped fiber ring laser cavity loss configuration for the chaos message masking scheme is carried out to optimize the generation of high quality chaos. A threefold increase in Lyapunov exponent implying higher security, and a significant increase in chaos bandwidth is achieved, both ideal for secure optical communication and nonlinear chaotic applications. The pulsed chaos is chaotic in a pulse time interval in addition to the amplitude resulting in better concealment of data pulses in a time domain. The chaos spectrum is a flat broadband and rich in spikes making spectral detection of a message more difficult. The range of five key parameters for which erbium-doped fiber ring laser retains its chaotic behaviour is also increased significantly reducing the effectiveness of a brute force attack to guess the erbium-doped fiber ring laser parameters. The chaos message masking scheme provides a higher security in comparison with additive chaos modulation scheme for implementation of chaotic optical communication using erbium- doped fiber ring laser. The security of a complete end-to-end chaotic optical communication system is tested by launching a spectral attack to estimate the message signal. The message signal clearly hides in a stronger chaotic signal and its spectral contents are not discernible.

Keywords: erbium-doped fiber ring laser chaos, optical chaos, chaos message masking, Lyapunov exponent, secure optical communication.

1. Introduction

Secure optical communication based on optical chaos in semiconductor lasers [1, 2] and on the use of loop nonlinearities [3] or periodically perturbing pump power [4] and cavity loss [5–10] in erbium-doped fiber ring laser (EDFRL) has been an area of interest for more than two decades now. It is emphasized that EDFRLs despite having a lesser chaos bandwidth as compared to semiconductor lasers, have three competitive advantages over semiconductor lasers in making a secure optical system using chaos:

i) EDFRL parameters are more flexible to be modified in the field without re-entering to the manufacturing loop,

ii) the dynamics of EDFRL is richer and can be better controlled,

iii) extra optical elements can be added into EDFRL loop to generate new types of chaos thus making this system more secure.

Cavity loss modulation based chaos generation scheme in EDFRL was studied by LUO and CHU [5] and later studied in detail by IMAI *et al*. [6] and ALI *et al*. [7]. The detailed study of changes in EDFRL chaos dynamics with parametric changes and changes in driving the loss modulation signal was done in an earlier work [7]. Later it was shown that the degree of chaos could be enhanced substantially by making the loss modulation signal more complex than just a pure sine wave [8]. However, in both these works [7, 8], the message signal was part of the loop with fixed amplitude and frequency; thus making these schemes a true additive chaos modulation (ACM) instead of initially perceived CMA/CMS [5], as corrected in a later work [10]. The effects of changes in message parameters on the chaos dynamics were studied in detail [10]. It was discovered [10] that in true ACM message amplitude, frequency and phase do change the chaos dynamics so much so that the output becomes non-chaotic if message frequency is integer multiple or sub-multiple of loss modulation frequency.

However, there were three main limitations of earlier ACM configuration [5, 7] which constrained its practical utilization in an end–end secure communication system. Firstly, the chaos pulses were chaotic in amplitude but periodic in time with same time period as of the modulating signal revealing the modulating frequency clearly in the spectral domain. Secondly, the highest frequency at which chaos was produced was limited. Thirdly, the range of parameters for which chaos was produced was less as the cavity switched to a periodic regime. The present chaos which is generated in chaos message masking (CMS) configuration removing message from the loop overcomes the above three limitations. The pulses in the current scheme are not only chaotic in amplitude but chaotic in time also. Since the chaos is produced using higher modulating frequencies and the pulses are chaotically placed in time, the resulting chaos has a higher bandwidth and is rich in frequency spectrum. Also the cavity remains in the chaotic region for a wider range of cavity parameters as compared to ACM scheme.

The objective of this work is to conduct the detailed dynamical analysis of the loss modulated EDFRL CMS scheme and compare the characteristics of the resulting chaos with that of ACM. The two main practical concerns of end–end chaotic optical communication after achieving successful synchronization, *i.e*., maximization of bandwidth of the message which can be hidden in chaos and the overall security of the chaotic communication system is also addressed. The former is limited by the chaos bandwidth itself and the latter is limited by the level of unpredictability in chaos, as measured by Lyapunov exponent. The EDFRL configuration selected here provides higher Lyapunov exponent and enhanced bandwidth. Also it is shown that the transmitter parameters are adjustable such that the message is neither visible in the time domain nor it can be spectrally filtered out from chaos. One new advantage achieved here is improved frequency domain masking of message and loss modulating frequency lines in a richer chaos spectrum.

2. Mathematical model

The schematic for implementation of CMA/CMS in EDFRL using loss modulation is shown in Fig. 1. The message signal S_{in} has been eliminated from the loop to make a true CMA/CMS and the mathematical model is modified:

$$\dot{E}_{\text{LA}} = -k_{\text{a}} E_{\text{LA}} + g_{\text{a}} E_{\text{LA}} D_{\text{A}} + \xi_{\text{LA}} \tag{1}$$

$$\dot{D}_{\text{A}} = -\frac{1}{\tau}\left[(1 + I_{\text{PA}} + E_{\text{LA}}^2) D_{\text{A}} - I_{\text{PA}} + 1\right] \tag{2}$$

$$k_{\text{a}} = k_{\text{a0}}\left[1 + m_{\text{a}} \sin(\omega_{\text{a}} t)\right] \tag{3}$$

Now the message will not affect the chaos generation dynamics and will be added after the generation of chaos. Fourth order Runge–Kutta method is employed and a very small time step size of 1 ns is used to get best accuracy of results with sufficient simulation time of 15 ms to isolate any transient behaviour. It is cautioned here that the simulation output becomes misleading if a greater step size is used; while it does not become self evident from the waveform itself. The symbols used in Eqs. (1)–(3) and default values used for simulations in this work are the same as given in Table 1 of earlier work [7], with the exception of a message signal which is not present now and an extended range of parameters studied here.

The steady state analysis of Eqs. (1) and (2) respectively gives a relation of threshold pump power and relaxation oscillation frequency:

$$I_{\text{PA-th}} = \frac{g_{\text{a}} + k_{\text{a}}}{g_{\text{a}} - k_{\text{a}}} \tag{4}$$

$$\omega_{\text{rel}} = \sqrt{\left(\frac{I_{\text{PA}}}{I_{\text{PA-th}}} - 1\right)(g_{\text{a}} + k_{\text{a}})} \tag{5}$$

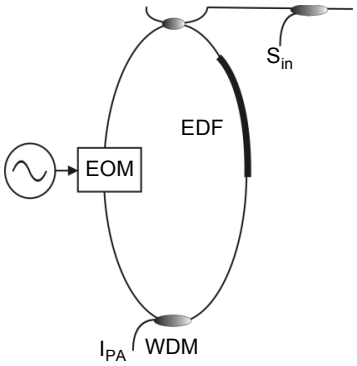

Fig. 1. Implementation of CMA/CMS in EDFRL using loss modulation. EDF – erbium-doped fiber, EOM – electro-optic modulator, WDM – wavelength division multiplexer (2 × 1 multiplexer for 980 nm pump power and 1550 nm loop lasing field), S_{in} – message signal , and I_{PA} – pump power.

3. Simulations

3.1. Effect of modulation index m_a

The modulation index is increased gradually from 0 to 1 and the significant results are plotted in Figs. 2**a** to 2**f**. Once $m_a = 0$, cavity loss is not modulated at all, the output

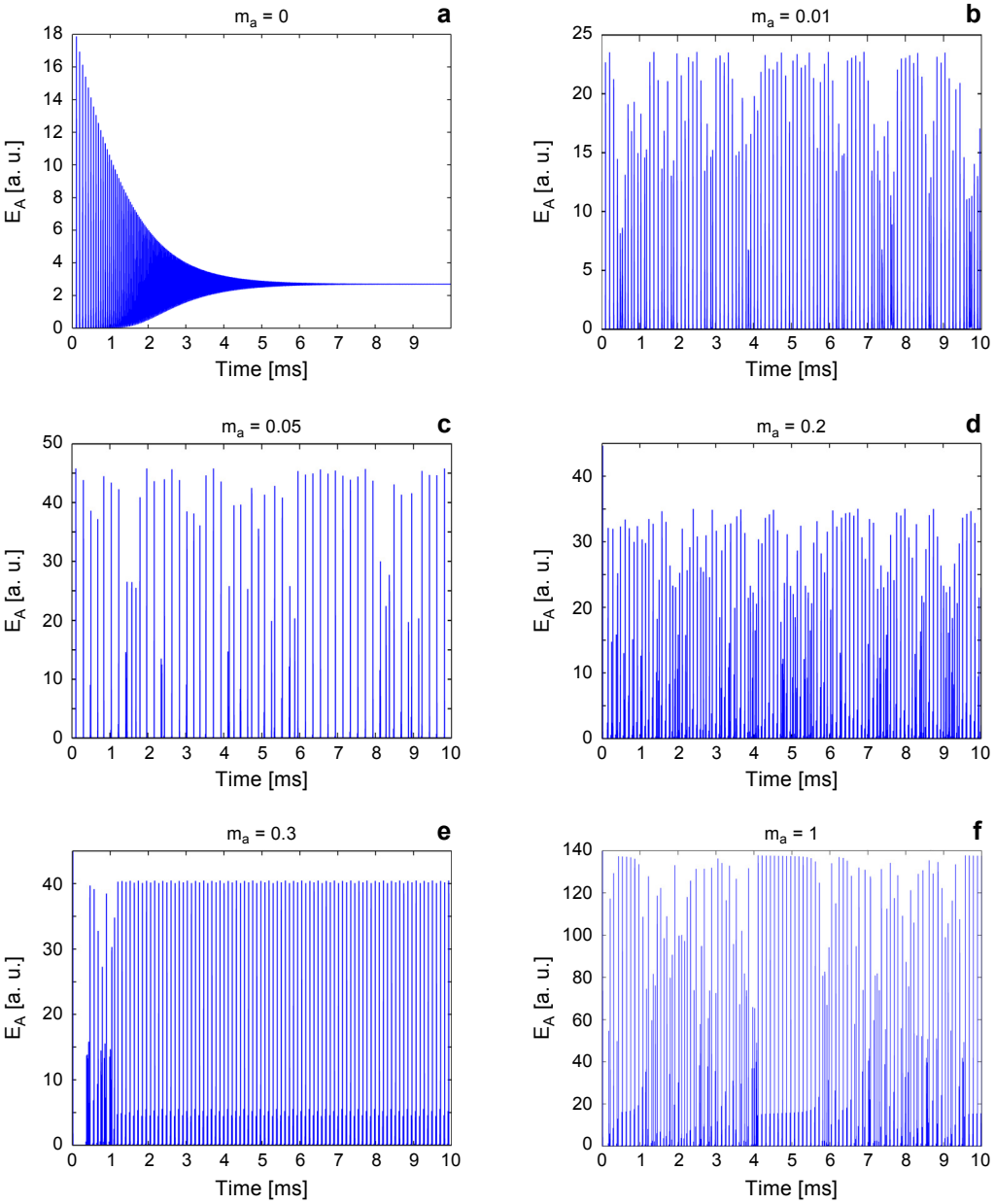

Fig. 2. Modulation index m_a variation: 0 (**a**), 0.01 (**b**), 0.05 (**c**), 0.2 (**d**), 0.3 (**e**), and 1 (**f**).

becomes steady with minor oscillations after an initial relaxation oscillation period as shown in Fig. 2**a**. It can also be observed that the pulses are getting smaller and closer to each other during a relaxation oscillation period. At a very small modulation index of 0.01, the output is chaotic as shown in Fig. 2**b** with interleaved bunches of high and low amplitude chaos, the latter with increased pulse repetition frequency. The switching between low and high amplitude clusters is observed at irregular intervals as shown in Fig. 2**c** for $m_a = 0.05$. The average amplitude of the chaotic pulses rises as the modulation index is increased to 0.2 as shown in Fig. 2**d**. The output becomes periodic at $m_a = 0.3$ as shown in Fig. 2**e**. The output again becomes chaotic above $m_a = 0.3$ (not shown for brevity) till it becomes intermittent chaos $m_a = 1$ as shown in Fig. 2**f**.

3.2. Effect of cavity loss k_{a0}

The default value being 3.3×10^7, k_{a0} is increased from 1.32×10^7 to 5.28×10^7 and some important results are shown in Figs. 3**a** to 3**f**. It is observed that the average frequency of chaotic pulses increases while their average amplitude decreases with the decrease of cavity loss. However, the output remains chaotic in time as well as ampli-

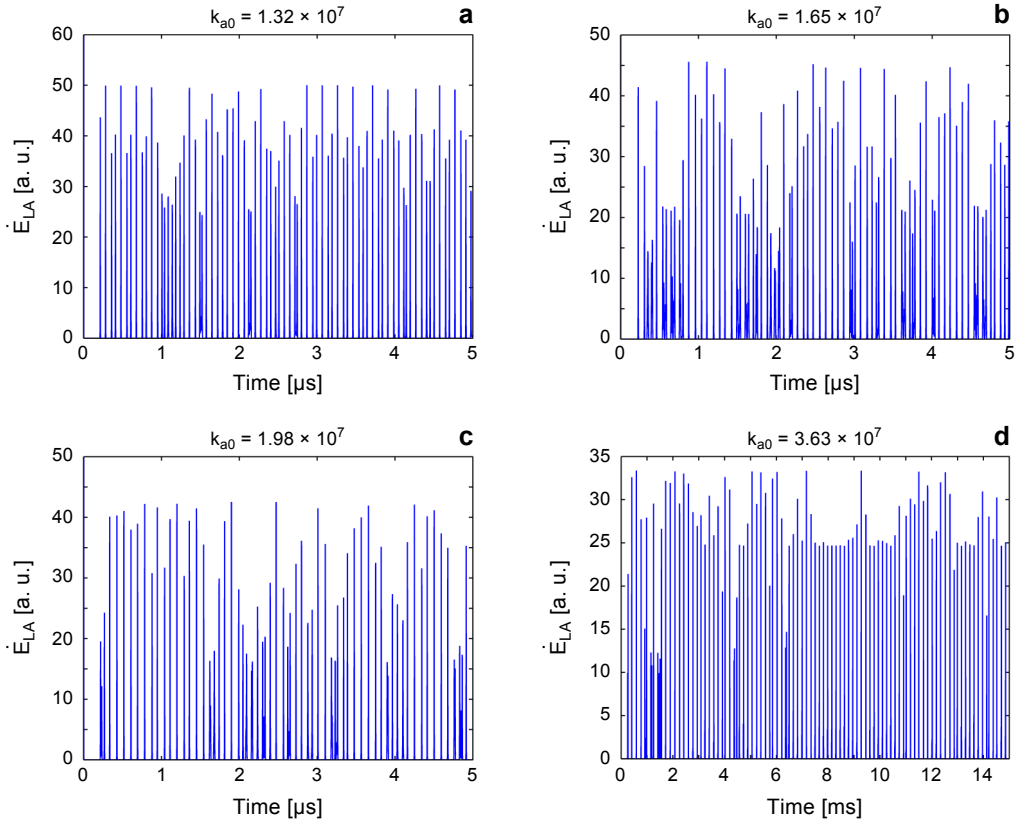

Fig. 3. To be continued on the next page.

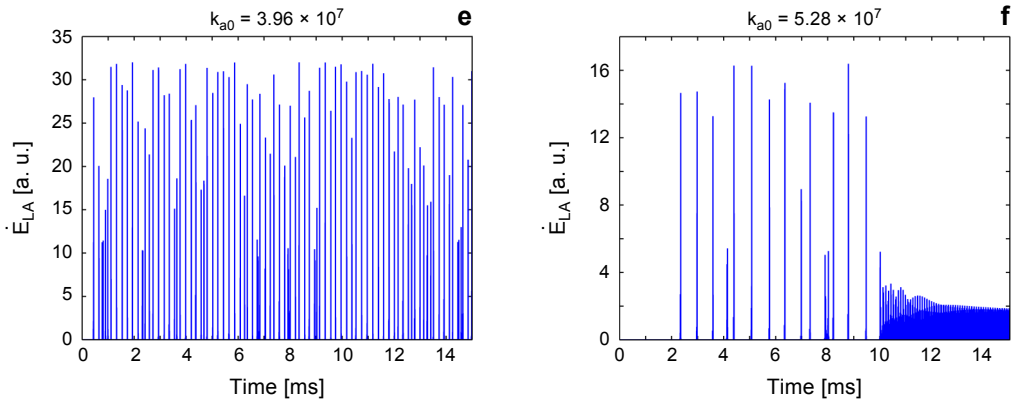

Fig. 3. Cavity loss k_{a0} variation: 1.32×10^7 (**a**), 1.65×10^7 (**b**), 1.98×10^7 (**c**), 3.63×10^7 (**d**), 3.96×10^7 (**e**), and 5.28×10^7 (**f**).

tude. It can be seen in Fig. 3**f** that the output becomes periodic after a transient exponential decay in pulses amplitude with the transient decay time decreasing with a decrease in cavity loss. Finally, the cavity switches to the periodic region of operation as was observed earlier also for ACM [7].

3.3. Effect of cavity gain g_a

The default value of the cavity gain is 6.6×10^7 which is twice the default cavity loss being sufficient to achieve a lasing action. For subject study, the cavity gain is increased from 5.61×10^7 to 2.64×10^8 and main results are shown in Figs. 4**a** to 4**f**. At two points, the output becomes 2-*T* periodic as obvious in Figs. 4**d** and 4**f**. Also the chaos approaches intermittency with periodic pulsing interleaved with chaos due to saturation of the cavity in Fig. 4**b**. It is observed that the "average amplitude" and

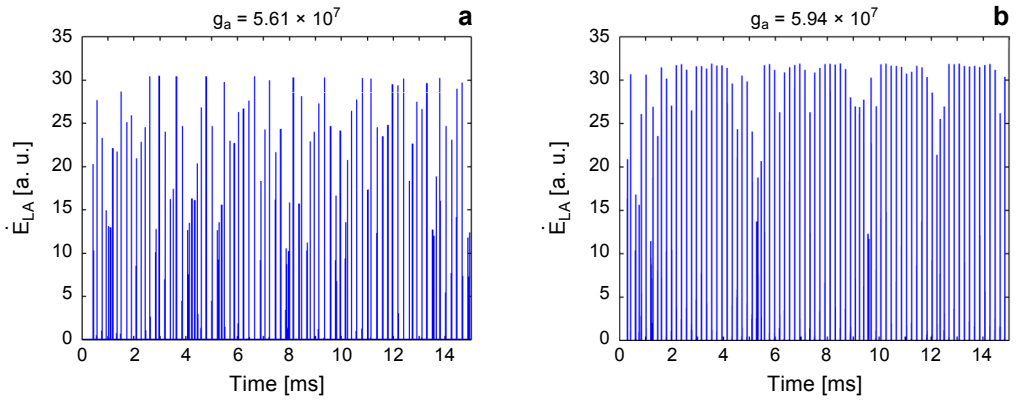

Fig. 4. To be continued on the next page.

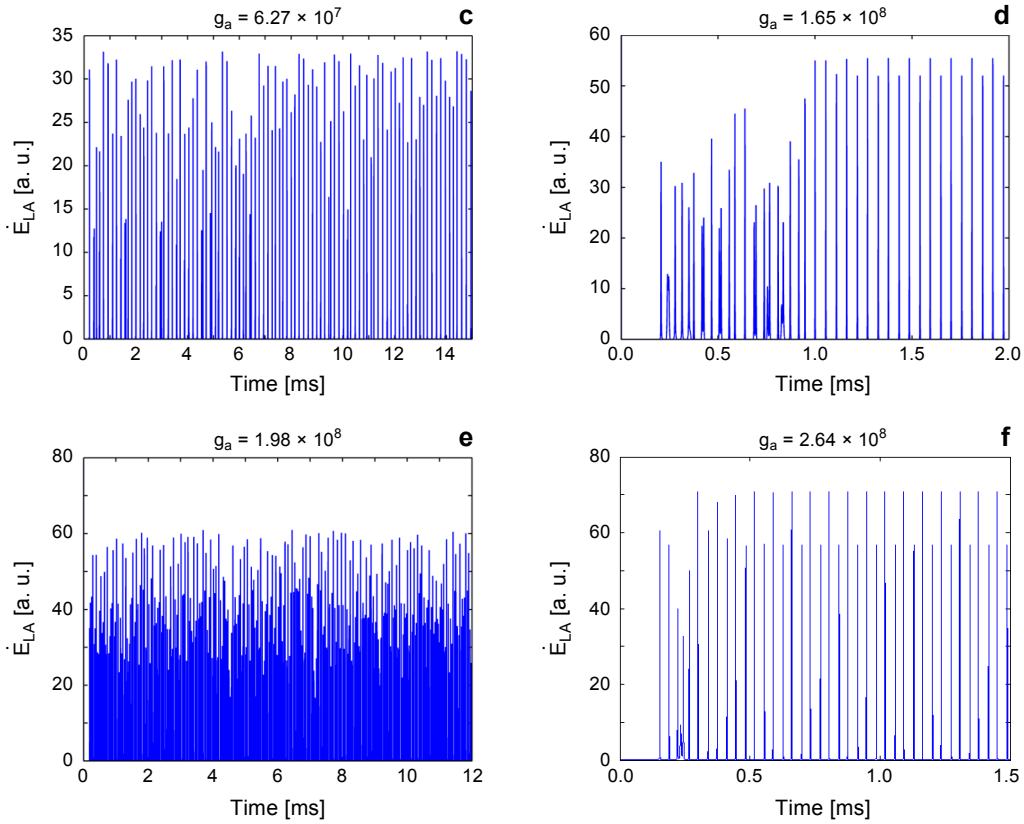

Fig. 4. Cavity gain g_a variation: 5.61×10^7 (**a**), 5.94×10^7 (**b**), 6.27×10^7 (**c**), 1.65×10^8 (**d**), 1.98×10^8 (**e**), and 2.64×10^8 (**f**).

"average frequency" of chaotic pulses increase with the increase in gain as the cavity has increased the number of erbium atoms energized to amplify photons with an increase in gain.

3.4. Effect of pump power I_{PA}

The pump power is increased from 10 to 100 mW and the significant results are plotted in Figs. 5**a** to 5**f**. The output becomes periodic for I_{PA} = 20 mW after a transient chaos of approximately 3 ms as shown in Fig. 5**b**. It can be observed from Fig. 5**c** that the pulses get closer as the pump power increases because population inversion is being achieved at a faster rate which in turn increases a pulse firing rate. The output becomes 2-*T* periodic at I_{PA} = 60 mW after a transient chaos of 0.15 ms as shown in Fig. 5**d** which is plotted on a smaller time scale till 1 ms only for clarity. The output again becomes chaotic above this level as one instance is shown at I_{PA} = 70 mW with much higher average pulse rate and increased average amplitude. The maximum amplitude

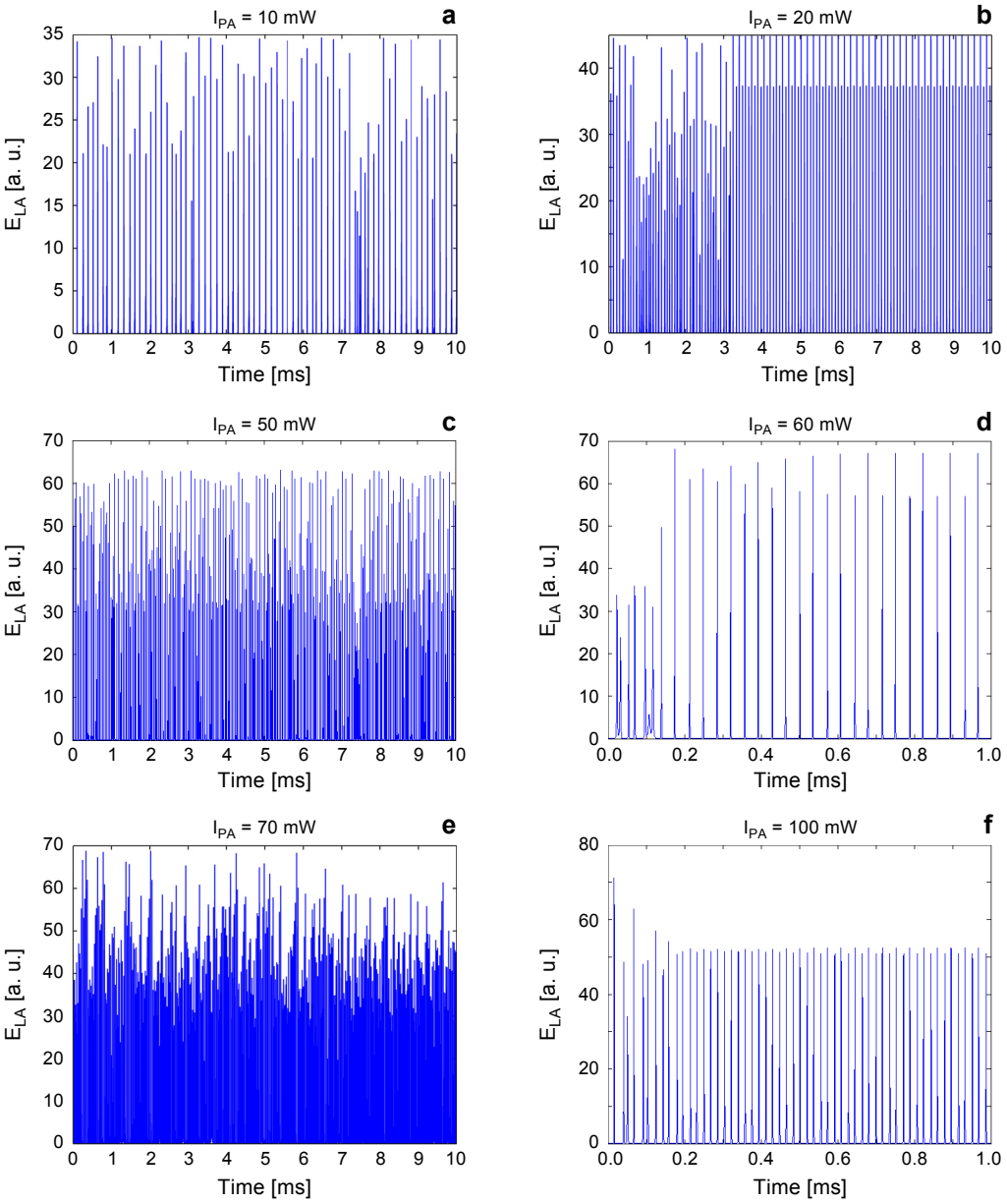

Fig. 5. Pump power I_{PA} variation: 10 (**a**), 20 (**b**), 50 (**c**), 60 (**d**), 70 (**e**), and 100 mW (**f**).

of pulses and the number of high amplitude pulses increase with the increase in pump power which is logical since the cavity gets more energy from the pump in any given time. There is a saturation effect observed in the amplitude of chaotic pulses due to gain saturation of the cavity and the output becomes 2-*T* periodic ultimately as shown in Fig. 5**f** for I_{PA} = 100 mW.

3.5. Effect of modulating frequency ω_a

The default modulating frequency being 3.5×10^5, here is increased from 10% of default, *i.e.* 3.5×10^4, to 10 times of default, *i.e.* 3.5×10^6, and significant results are shown in Figs. 6**a** to 6**f**. The output remains chaotic over a very broad range of ω_a as

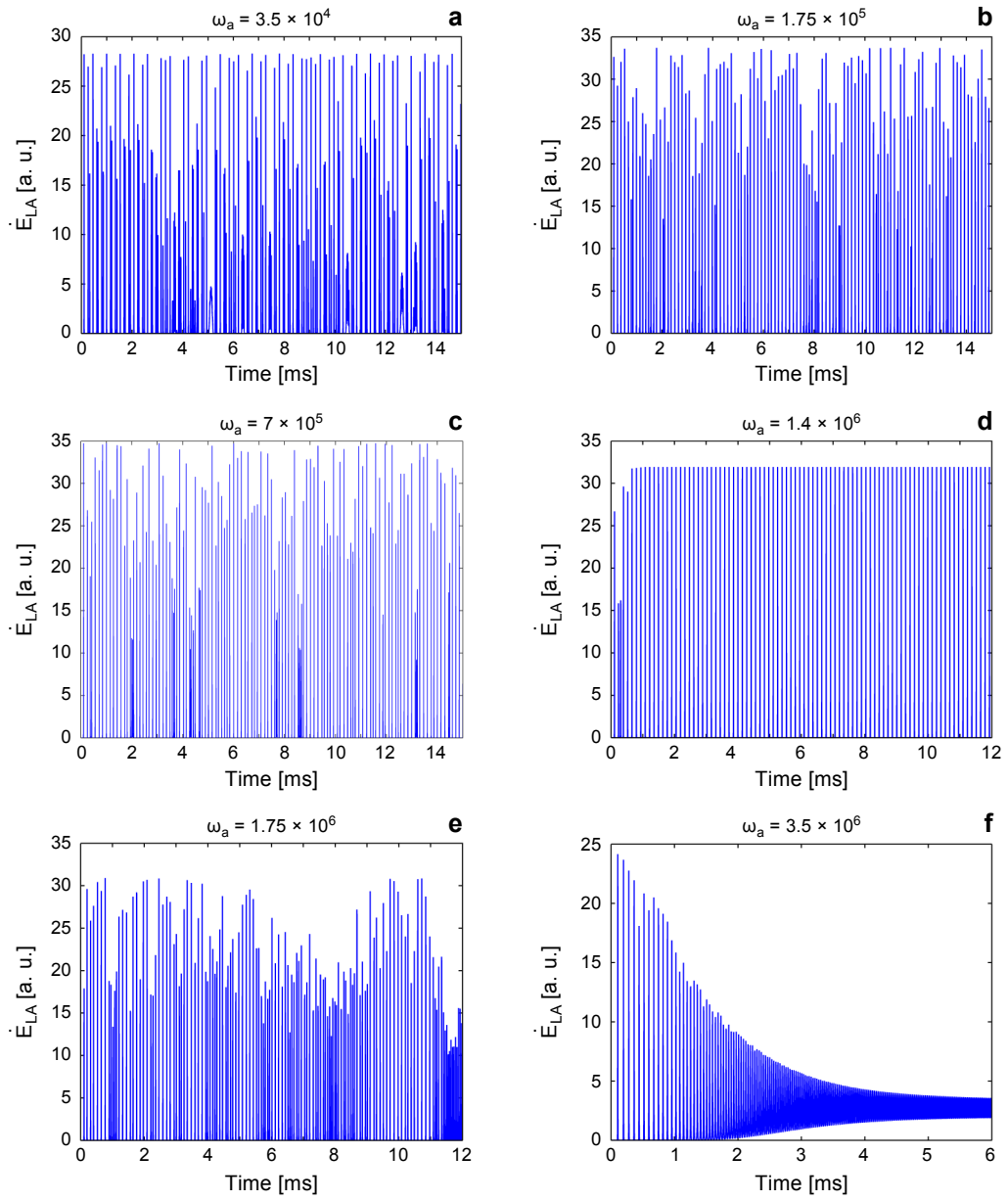

Fig. 6. Modulating frequency ω_a variation: 3.5×10^4 (**a**), 1.75×10^5 (**b**), 7×10^5 (**c**), 1.4×10^6 (**d**), 1.75×10^6 (**e**), and 3.5×10^6 (**f**).

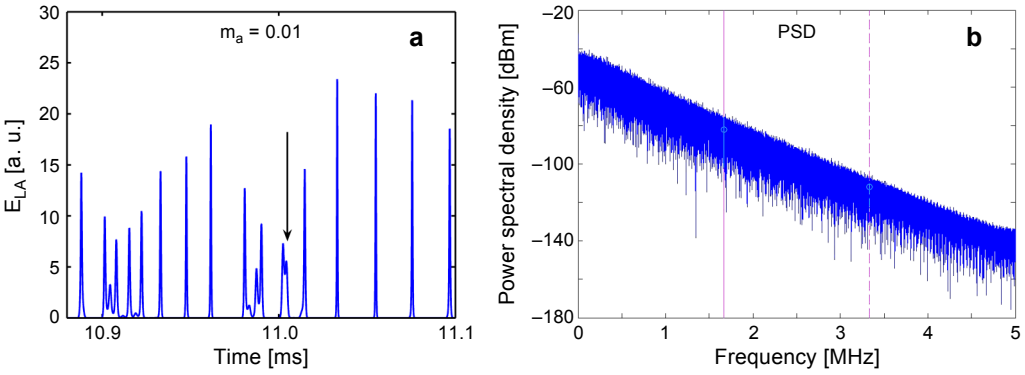

Fig. 7. Time and frequency waveforms. Gaussian pulses merging at some points (**a**). Flat broadband frequency spectrum (**b**).

is obvious from Figs. 6**a** to 6**e** with a few exceptions like in Fig. 6**d** where it becomes periodic and Fig. 6**f** where it decays exponentially to a smaller oscillatory behaviour. It can be observed in general that pulses get smaller and closer as the modulating frequency is increased because of the limitation in available cavity energy. In order to regain chaos at higher modulating frequencies, pump power or cavity gain has to be increased but it cannot be done indefinitely since the output becomes first periodic and then steady as we increase these two parameters.

3.6. Waveform analysis

The individual pulses are still Gaussian but without humps as compared to [7] and also sometimes merged together due to chaotic placement in time as shown in Fig. 7**a** (arrow indicating two pulses merged), which is zoomed in version of Fig. 2**b** at $m_a = 0.01$. The frequency spectrum for default parameters is flatter and enriched in spectral lines as shown in Fig. 7**b** without the modulating spectral line being prominent. The maximum LE using TISEAN is now found increased to 0.74769 for chaos of Fig. 5**e**, *i.e.* $I_{PA} = 70$ mW with rest default parameters. This LE value is three times better than earlier work reported [7, 10] where maximum LE shown was 0.25. It is known that [11] chaotic signals do not follow usual 3-dB spectrum definitions and the effective bandwidth is measured by measuring the bandwidth from DC to the frequency where 80% of the power resides. Applying 80% energy definition, the bandwidth of chaos spectrum found here is approximately 2 MHz, which is more than in previous work [7]. Also the spectral lines have increased and the spectrum has become flatter, which increases the message hiding ability in the frequency domain.

4. CMS advantages

The above results show significant improvements in the retention of the chaotic mode of operation for an increased range of parameters as compared to the reported results.

The limitation of ACM chaos being periodic in time is successfully removed by shifting to CMS scheme and the pulses are chaotic in time in addition to being chaotic in amplitude. The pulses remain Gaussian and their width become much narrow which also increases the bandwidth of chaos. The humps beneath the pulses have disappeared for all values of the modulation index. Two-pulse merging and three-pulse merging are also observed occasionally in this work as shown in simulations, which is a good sign as it increases unpredictability of chaos. Instead of bunching, there are groups of low and high amplitude pulses interleaved with each other. The chaotic pulses appear in the form of denser and rarer bunches now with low and high average amplitudes respectively, in an interleaved fashion. However, they still maintain their behaviours of a chaotic peak amplitude and a chaotic interval on a pulse to pulse basis which is a must for a secure communication system application.

As the cavity is being pumped continuously with fixed pump power, there is an upper limit to the total energy released in a given interval from the cavity in the form of chaotic pulses. Consequently, chaotic pulses with a lower average amplitude occur more frequently while the higher amplitude cluster has increased an inter-pulse interval. However, if the pump power is increased sufficiently, most of the chaotic pulses saturate to limiting the maximum amplitude and the output becomes periodic with 2-*T* and then 1-T periodic pulsing. The Lyapunov exponents are increased as compared to the previously reported work by as much as three times. The chaos has a flat broadband spectrum which implies that the message concealment increases spectrally. It was shown by YANHUA HONG *et al*. [12] that a flat broadband response of a chaotic signal is a more desirable feature from the application point of view as compared to the opposite case.

5. End-to-end CMS system

An end-to-end chaotic optical communication system based on CMS scheme is shown in Fig. 8. The message is added to the transmitter generated chaos and sent over the

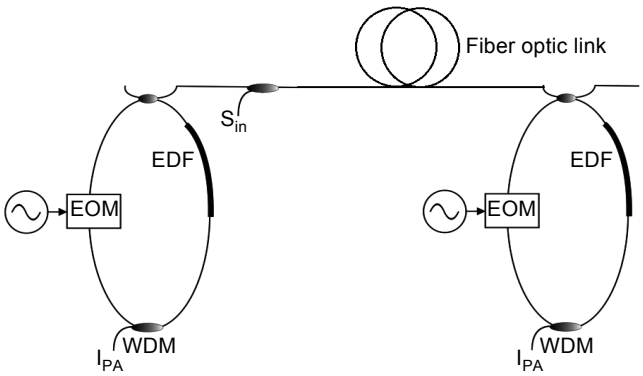

Fig. 8. End–end communication using CMS. EDF – erbium-doped fiber, EOM – electrooptic modulator, WDM – wavelength division multiplexer, S_{in} – message signal , and I_{PA} – pump power.

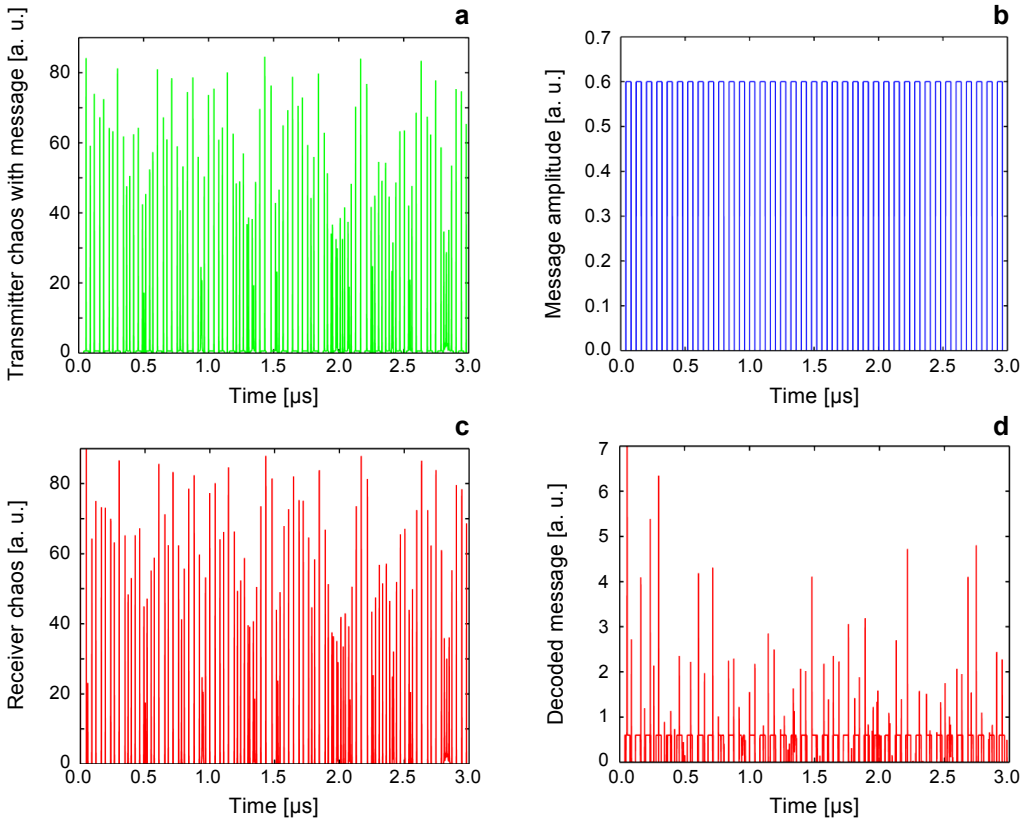

Fig. 9. Time domain waveforms of end-to-end CMS system. Transmitted chaos with message added (**a**), message signal (**b**), receiver generated synchronised chaos (**c**), and decoded message after subtraction (with noise) (**d**).

fiber optic link to the receiver. The receiver loop is synchronised to the transmitter chaos using a seed from the transmitter with a coupling ratio of 0.02. The receiver generated synchronised chaos is subtracted from the received chaos plus message signal (the subtraction process is not shown).

The waveforms at different test points of the end-to-end CMS system are shown in Fig. 9. The transmitter chaos containing the message signal is shown in Fig. 9**a**. The message signal is a square wave as shown in Fig. 9**b**. The message amplitude is order of magnitude less than chaotic pulses and is masked by the chaos fully; hence the name chaos message masking is used for this type of chaos message encoding. The receiver generated chaos which can be minutely observed to get fully synchronised after 0.3 ms delay is shown in Fig. 9**c**. The decoded message after subtracting the receiver generated synchronised chaos from the total received signal is shown in Fig. 9**d**. The spikes seen in the recovered message are because of the synchronisation occasional mismatches due to the two realisations of chaos being slightly different in amplitude. These spikes can be easily filtered out using a low pass filter. It may be noted that

fiber optic link distortions have not been simulated here as detailed independent studies were carried out earlier in a dispersion and nonlinearities effects study for a single channel [13] and Raman effect study for eight DWDM channels [14].

6. Security analysis of CMS scheme

The sync diagram between the transmitter and receiver chaos for different scenarios is shown in Fig. 10. When transmitter and receiver loop parameters are identical, the sync diagram is shown in Fig. 10**a**. In case of receiver modulating frequency different from that of the transmitter by only 1%, the synchronisation error is shown in Fig. 10**b**. This proves that it is very difficult to break chaos security till an exact value of modulating frequency is matched. Similarly, the security will further improve if we add the phase of the modulating signal as an additional parameter. For the rest of the five loop parameters as reported by LUO and CHU [5], an allowance of 5% deviation in the receiver and transmitter parameters values will be studied in detail in our next work. The sync diagram of Fig. 10**a** is still having a spread in the centre of the ellipse and it

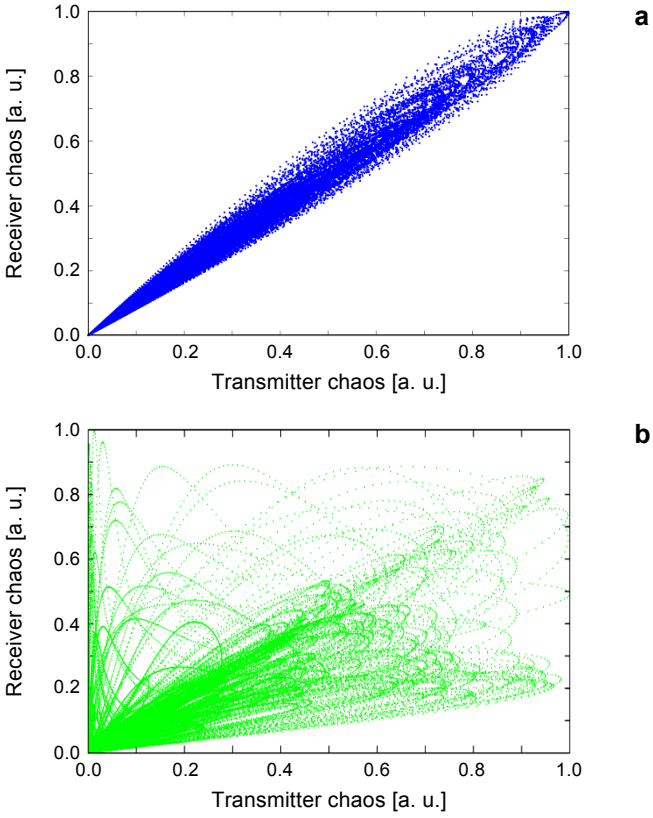

Fig. 10. Deviation of sync diagram with parameters: 100% parameters matched (**a**) and 1% deviation in modulating frequency (**b**).

is not a straight line because the receiver is getting an extra signal in the loop consisting of transmitter chaos and the message added before transmission. While 2% of this seed is a must for synchronisation, it deviates the amplitude of receiver chaos pulses slightly causing the observed spread in Fig. 10**a**.

Despite showing above that the security offered by keeping secrecy of transmitter five parameters values is quite robust as shown by the sync diagram, we have gone one step ahead to study the spectral attack possibility. The spectra of transmitted chaos without and with a message are shown respectively in Figs. 11**a** and 11**b** to study the possibility of success of a spectral attack by an intruder. Since the message amplitude is kept very low as compared to chaos, the message frequency is not visible in Fig. 11**b** and hence cannot be simply filtered out. However, some higher harmonics are visible at the extreme right end of Fig. 11**b** because we added a square wave message which has a sinc waveform Fourier series. Still it cannot reveal any information because of two reasons, *i.e.*, harmonics visible are 60 dB down the main signal and these will keep

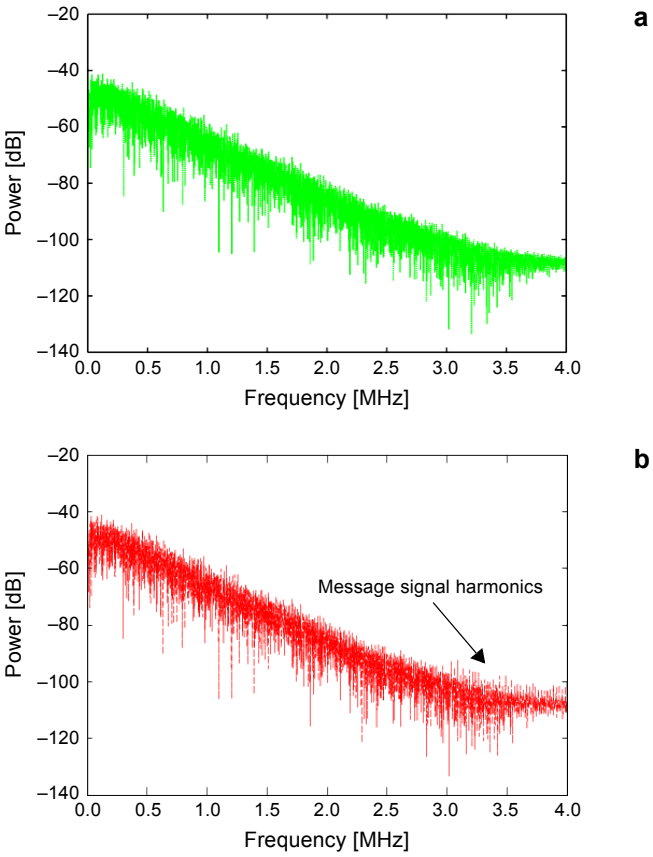

Fig. 11. Message remains hidden during spectral attack. Transmitted chaos spectrum without (**a**) and with (**b**) message.

varying in position and frequency as we mask a pseudo-random binary message in a real scenario instead of a plain square wave here.

7. Conclusions

The optimization of chaos parameters results in the improved signature in time and frequency domains with increased security and control on generation of chaos using CMS scheme in the cavity loss modulation of EDFRL. The three improvements in a chaotic signature which directly translate into increased chaotic communication security are outlined here. Firstly, the system retains a chaotic mode of operation for a wider range of parameters reducing the risks of a brute force attack. Secondly, pulses are chaotic in a time interval in addition to being chaotic in amplitude, thus improving unpredictability of chaos and improved temporal message hiding. Thirdly, chaos has a flat broadband shape and it varies with all five key parameters instead of just the modulation frequency reducing the risks of a spectral analysis attack. The optimized chaos is chaotic in time as well as in amplitude. The chaos pulses are still Gaussian but with skew and humps removed as compared to ACM behaviour. This in turn helps spectrally masking both modulating and message frequencies in the frequency domain. The Lyapunov exponent is raised by three times which is a logical consequence of all the above mentioned improvements in a chaos signature. This increases the unpredictability of chaos and security of EDFRL chaos communication system by three times. The end-to-end simulation of CMS system signifies the success of CMS scheme in masking the message in chaos and recovering it correctly. The spectral attack on a chaos plus message is found unable to segregate the message form chaos. Also the system is so sensitive to some parameters like modulating frequency that a 1% guessing error results in the total loss of synchronisation as shown in the results. Besides communication security, the new results found here are also of a great value from nonlinear dynamics, random number generation and LIDAR point of views, as EDFRL is rich in dynamics nonlinear platform.

References

[1] Virte M., Panajotov K., Thienpont H., Sciamanna M., *Deterministic polarization chaos from a laser diode*, Nature Photonics **7**(1), 2013, pp. 60–65.

[2] Argyris A., Syvridis D., Larger L., Annovazzi-Lodi V., Colet P., Fischer I., García-Ojalvo J., Mirasso C.R., Pesquera L., Shore K.A., *Chaos-based communications at high bit rates using commercial fibre-optic links*, Nature **438**(7066), 2005, pp. 343–346.

[3] Abarbanel H.D.I., Kennel M.B., Buhl M., Lewis C.T., *Chaotic dynamics in erbium-doped fiber ring lasers*, Physical Review A **60**(3), 1999, pp. 2360–2374.

[4] Pisarchik A.N., Kir'yanov A.V., Barmenkov Y.O., Jaimes-Reátegui R., *Dynamics of an erbium-doped fiber laser with pump modulation: theory and experiment*, Journal of the Optical Society of America B **22**(10), 2005, pp. 2107–2114.

[5] Luo L.G., Chu P.L., *Optical secure communications with chaotic erbium-doped fiber lasers*, Journal of the Optical Society of America B **15**(10), 1998, pp. 2524–2530.

[6] IMAI Y., MURAKAWA H., IMOTO T., *Chaos synchronisation characteristics in erbium-doped fiber laser systems*, Optics Communications **217**(1–6), 2003, pp. 415–420.
[7] ALI S.Z., ISLAM M.K., ZAFRULLAH M., *Effect of parametric variation on generation and enhancement of chaos in erbium-doped fiber-ring lasers*, Optical Engineering **49**(10), 2010, article ID 105002.
[8] ALI S.Z., ISLAM M.K., ZAFRULLAH M., *Generation of higher degree chaos by controlling harmonics of the modulating signal in EDFRL*, Optik – International Journal for Light and Electron Optics **122**(21), 2011, pp. 1903–1909.
[9] ALI S.Z., ISLAM M.K., ZAFRULLAH M., *Comparative analysis of chaotic properties of optical chaos generators*, Optik – International Journal for Light and Electron Optics **123**(11), 2012, pp. 950–955.
[10] ALI S.Z., ISLAM M.K., ZAFRULLAH M., *Effect of message parameters in additive chaos modulation in erbium doped fiber ring laser (EDFRL)*, Optik – International Journal for Light and Electron Optics **124**(18), 2013, pp. 3746–3750.
[11] FAN-YI LIN, YUH-KWEI CHAO, TSUNG-CHIEH WU, *Effective bandwidths of broadband chaotic signals*, IEEE Journal of Quantum Electronics **48**(8), 2012, pp. 1010–1014.
[12] YANHUA HONG, SPENCER P.S., SHORE K.A., *Flat broadband chaos in vertical-cavity surface-emitting lasers subject to chaotic optical injection*, IEEE Journal of Quantum Electronics **48**(12), 2012, pp. 1536–1541.
[13] ALI S.Z., ISLAM M.K., ZAFRULLAH M., *Effect of transmission fiber and amplifier noise on optical chaos synchronization*, Optical Review **19**(5), 2012, pp. 320–327.
[14] ALI S.Z., ISLAM M.K., ZAFRULLAH M., *Effect of transmission fiber on dense wavelength division multiplexed (DWDM) chaos synchronization*, Optik – International Journal for Light and Electron Optics **124**(12), 2013, pp. 1108–1112.

Received November 13, 2016
in revised form February 7, 2017